Importance of Spin-Orbit Effects in Parity-Unfavored Photoionization of Neon, Observed Using a Two-Dimensional Photoelectron Imaging Technique

A. A. Wills,[1,*] T. W. Gorczyca,[1] N. Berrah,[1] B. Langer,[2] Z. Felfli,[3] E. Kukk,[1,4] J. D. Bozek,[4] O. Nayandin,[1] and M. Alshehri[1]

[1]*Department of Physics, Western Michigan University, Kalamazoo, Michigan 49008-5151*

[2]*Fritz-Haber-Institut der Max-Planck-Gesellschaft, Faradayweg 4-6, D-14195, Berlin, Germany*

[3]*Center for Theoretical Studies of Physical Systems, Clark Atlanta University, Atlanta, Georgia 30314*

[4]*Lawrence Berkeley National Laboratory, Advanced Light Source, University of California, Berkeley, California 97420*

(Received 5 November 1997)

We present an experimental and theoretical study of photoexcitation and decay mechanisms of doubly excited resonances in neon. New spin-orbit induced effects are identified in the angle-resolved and photoelectron-resolved differential cross sections for a parity-unfavored transition. These observations are facilitated using a two-dimensional imaging technique, and highlight the importance of considering spin-orbit induced effects when studying detailed spectra in atomic systems as light as neon. [S0031-9007(98)06291-7]

PACS numbers: 32.80.Fb, 31.25.–v, 31.50.+w, 32.80.Dz

The simultaneous excitation of two atomic electrons by a single photon has been the subject of numerous experimental and theoretical investigations. These intermediate resonance states reveal higher-order, interelectron correlation effects, and provide a more stringent testing ground for the accuracy of existing theoretical and computational methods. Helium, due to its relative simplicity, has been studied extensively [1]. The case of neon, however, is more complicated than helium due to the occupied $2p$ subshell, which leads to a dense grouping of the Ne^+ $2p^4nl$ states and hence more complex resonances. Nevertheless, many studies have been performed on this system as well, and some have observed spin-orbit effects. Early photoabsorption results demonstrated departure from LS-coupling predictions (i.e., the neglect of spin-orbit effects), by observing the fine-structure splittings of the $2p^4(^3P)3s(^2P_{1/2,3/2})nl$ resonances [2]. Later measurements [3–5] were able to observe additional spin-orbit effects by detecting resonance contributions in the photoionization excitation to quartet ionic states, which is a forbidden process in LS coupling. More recently, the fine-structure splitting of resonance series was observed in greater detail [6] than was possible in the earlier studies [2]. These results established the existence of certain spin-orbit effects in the photoionization of neon, but they lacked additional information provided by highly differential measurements. Furthermore, in the earlier cases, only *small* spin-orbit corrections were observed.

The purpose of the present Letter is to demonstrate that for certain neon resonances, the angular distribution of photoelectrons and the ratio of partial cross sections to individual fine-structure levels both exhibit behavior that deviates markedly from LS-coupling predictions. Such observations provide further quantitative determination of the breakdown of LS coupling. Particular attention will be given to the $2p^43pns, nd$ doubly excited resonances in photoionization excitation to the Ne^+ $2p^4(^3P)3s(^2P)$ state. These findings were achieved using high-resolution measurements of photoionization cross sections that are differential in photon energy, photoelectron energy, and photoelectron angle.

The $2p^43pns, nd$ resonances are particularly strong because the $\sim$10% mixing of the $2p^53p$ configuration in the $2p^6$ ground state leads to the one-electron photoexcitation $2p^53p \rightarrow 2p^43pns, nd$ [6]. Breakdown of LS coupling for this light system is due to the spin-orbit interaction, which, as we will discuss, most likely causes mixing between certain LS-allowed $2p^43pns, nd(^1P_1)$ resonances and their $^3S_1$, $^3P_1$, and $^3D_1$ LS-forbidden counterparts. Angle-resolved and level-resolved measurements can provide a signature of these spin-orbit effects, which we will first discuss from a theoretical standpoint before presenting the experimental results.

For linearly polarized light, the differential photoionization cross section as a function of θ (the angle between the photoelectron momentum vector and the photon polarization axis) takes the analytic form [7]

$$\frac{d\sigma}{d\Omega} = \frac{\sigma}{4\pi}[1 + \beta P_2(\cos\theta)], \tag{1}$$

thereby defining the angular distribution parameter β. A particularly useful way of viewing the underlying dynamics incorporated in $\frac{d\sigma}{d\Omega}$ is to consider the angular momentum transfer $\vec{j}_t$ [8]. For photoionization, an incident photon of angular momentum $\vec{j}_\gamma$ ($j_\gamma = 1$) is absorbed by an initial atomic state of total angular momentum $\vec{J}_0$, producing a photoelectron of orbital angular momentum $\vec{\ell}$ coupled to the residual system (the final ionic state plus the *unobserved* photoelectron spin) of total angular momentum $\vec{J}_c$. The angular momentum transfer $\vec{j}_t = \vec{j}_\gamma - \vec{\ell} = \vec{J}_c - \vec{J}_0$ is a useful quantity because the differential cross

section reduces to an incoherent sum of terms associated with the allowed values of j_t [8]; these are $j_t = \ell - 1, \ell, \ell + 1$ by the first triangular inequality, and may be further restricted by the second triangular inequality $|J_c - J_0| \leq j_t \leq J_c + J_0$. While the *parity-favored* contributions $j_t = \ell \pm 1$ have complicated, energy-dependent angular distributions in general, the partial differential cross sections for all *parity-unfavored* transitions $j_t = \ell$ have the analytic property $(\frac{d\sigma}{d\Omega})_{j_t=\ell} \propto \sin^2\theta$ independent of energy, or equivalently, $\beta_{\text{unf}} = -1$ [9]. One important consequence is that the parity-unfavored contribution to the differential cross section vanishes at $\theta = 0°$.

For photoionization from the $2p^6(^1S)$ ground state to the $2p^4 3s(^2P)\epsilon p(^1P)$ continuum, the angular momentum transfer is restricted to the single, parity-unfavored value $j_t = \ell = 1$ in LS coupling, and the differential cross section vanishes at $\theta = 0°$. When spin-orbit effects are considered, on the other hand, L and S are not necessarily conserved (i.e., the final state may be one of the triplets $^3L_1$ instead), so that $j_t = \{0, 1, 2\}$ are all allowed values and the cross section does not necessarily vanish at $\theta = 0°$. Thus, detection of photoelectrons at $\theta = 0°$, which we will report, is an unmistakable indication of LS-coupling breakdown.

We have also found that a second LS-coupling prediction does not hold for certain resonances. In the absence of any spin-orbit effects, the $2p^4 3s(^2P)\epsilon p(^1P_1)$ final continuum decomposes, by statistical weights, into an admixture consisting of 2/3 of the $^2P_{3/2}\epsilon p_{1/2,3/2}$ and 1/3 of the $^2P_{1/2}\epsilon p_{1/2,3/2}$ $J = 1$ continua. Differential cross sections to these two levels should therefore assume the exact, energy-independent ratio $r = 2$ in LS coupling. By considering spin-orbit effects, on the other hand, and thus including mixing with the triplet final states, this ratio may fluctuate ($r \neq 2$). For example, photoexcitation of the $^3D_1$ resonances through spin-orbit mixing with the $^1P_1$ LS-allowed resonances enables autoionization to f-wave photoelectrons in the $^2P_{3/2}\epsilon f_{5/2}(^3D_1)$ state, and these photoelectrons cannot couple to the $^2P_{1/2}$ ionic level. Such differences between photoelectrons coupled to the $^2P_{3/2}$ and $^2P_{1/2}$ ionic levels can then lead to LS-forbidden ratios $r \neq 2$.

In order to easily observe the photoionization processes described above, we generated two-dimensional (photon energy and photoelectron energy) photoelectron spectra (2DPES) at two angles, shown in Fig. 1. The apparatus used consists of two highly efficient time of flight (TOF) electron energy analyzers positioned at $\theta = 0°$ and $\theta = 54.7°$ [10]. The measurements were performed on the high resolution atomic, molecular, and optical undulator beam line (9.0.1) at the Advanced Light Source at Lawrence Berkeley National Laboratory. The 2DPES were constructed from PES collected with the two TOF analyzers. The PES were allowed to accumulate simultaneously at the two angles for 10 s; then the photon energy was incremented by 6 meV. This was repeated until the photon energy range of interest was covered. All spectra shown have been corrected for variations in photon flux and the electron transmission efficiency of the analyzers as a function of kinetic energy. The photon energy scale was calibrated using the positions of several prominent doubly excited resonances, which were compared to previous photoionization data [6]. The photon energy resolution was set to 20 meV at 57 eV for the data shown, which is a significant improvement over the previous resolution of 100 meV in earlier differential measurements [3].

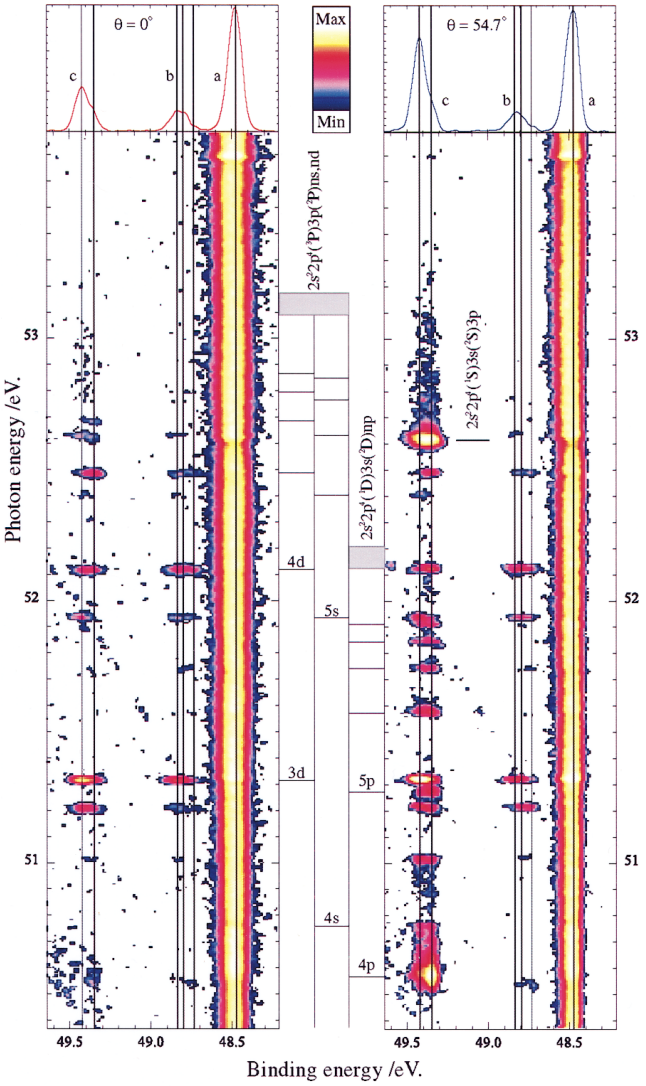

FIG. 1(color). Photoelectron yield as a function of photon energy and binding energy (photon energy minus photoelectron energy) at 0° and 54.7°. The upper graphs show the spectrum at 51.3 eV photon energy, and the vertical bars indicate the positions of the (a) $2s2p^6(^2S)$, (b) $2s^2 2p^4(^3P)3s(^4P)$, and (c) $2s^2 2p^4(^3P)3s(^2P)$ fine-structure levels.

By viewing the experimental results in this 2D manner, it is easy to observe new LS-forbidden features. First, the vertical lines (b) in Fig. 1 [corresponding to the $2p^4 3s(^4P_{J_c})$ satellites at 48.8 eV binding energy] show,

on certain resonances, noticeable photoelectron yields at both angles, indicating LS-coupling breakdown. Also by comparing the photoelectron yields at 54.7° and 0° along the vertical lines (c) in Fig. 1 [corresponding to the $2p^4 3s(^2P_{J_c})$ satellites at 49.4 eV], it can be seen that several resonances appear at both angles while others disappear in the 0° spectrum. For instance, the $2p^4(^3P)3p(^2P)3d$ resonance at (photon energy) 51.3 eV shows a photoelectron yield that is almost equally as strong at 0° as it is at 54.7°, whereas the $2p^4(^1D)3s(^2D)4p$ resonance at 50.6 eV disappears almost completely in the 0° spectrum. Since these are parity-unfavored transitions in LS coupling, the appearance of any signal at 0° is an immediate indication of the breakdown of LS coupling.

The high photoelectron-energy resolution allows easy identification of one additional LS-forbidden feature. By looking at the photoelectron intensity along the two vertical lines (c) in Fig. 1 corresponding to the $2p^4 3s(^2P_{3/2})$ and $2p^4 3s(^2P_{1/2})$ satellites (at 49.35 eV and 49.42 eV binding energies, respectively), it can clearly be seen that the ratio is not constant ($r \neq 2$). For instance, the $2p^4(^3P)3p(^2P)3d$ resonance shows a ratio $r \ll 2$, indicating a breakdown of LS coupling.

Having identified regions in which interesting spin-orbit effects occur, it is then possible to obtain the photoelectron yield along narrow vertical strips in Fig. 1 to produce more conventional one-dimensional plots of differential cross sections vs photon energy (see Figs. 2 and 3). Considering Eq. (1), the total photoelectron yield at each angle can be used to compute the angular distribution parameter $\beta = [\frac{d\sigma}{d\Omega}(0°)/\frac{d\sigma}{d\Omega}(54.7°)] - 1$. The results presented in Fig. 2 indicate more quantitatively that the $2p^4(^3P)3p(^2P)ns, nd$ resonances are essentially the only ones that show a nonzero cross section at 0° ($\beta > -1$); they further emphasize that spin-orbit effects play a *major* role in the process we are studying, causing substantial changes in β rather than just small perturbations. We attribute these changes to spin-orbit mixing between singlet and triplet resonances, as will be discussed below.

The extent to which a $^1P_1$ resonance state $|i\rangle$ and a triplet state $|j\rangle$, with LS-coupling energies E_i and E_j, mix via the spin-orbit operator H_{SO} is given in first-order perturbation theory as

$$\left| \frac{c_j}{c_i} \right|^2 \sim \left| \frac{\langle j|H_{\mathrm{SO}}|i\rangle}{E_j - E_i} \right|^2 . \qquad (2)$$

The strength of the spin-orbit operator is very weak in neon—on the order of 10 meV—so significant mixing occurs only between nearly degenerate states $E_i \sim E_j$. But since both singlet and triplet *resonances* converge to the same $2p^4(^3P)3p(^2P)$ ionic thresholds, these energies eventually approach each other as n increases, and therefore mix more readily. The constant nonzero yield at 0° in the 52.8–53.1 eV region in Fig. 2 is evidence of this. Similar deviations from the LS-predicted constant behavior $\beta = 2$ in the *parity-favored* $h\nu + 3s^2 \rightarrow 3s\epsilon p$ photoionization in magnesium were observed for the high-n Rydberg region [11]. However, the present observation of mixing in even the lowest $n = 3$ resonance at 51.3 eV is not expected.

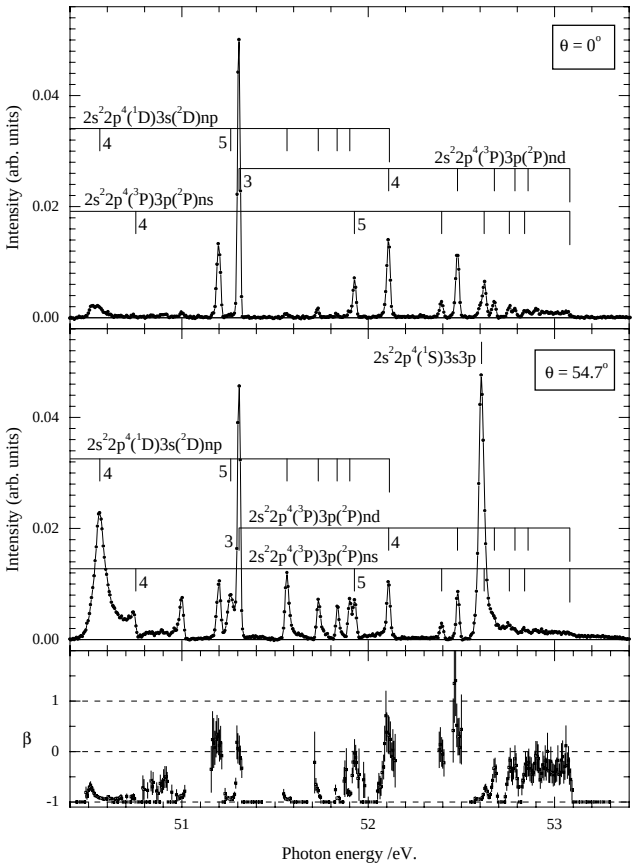

FIG. 2. Photoelectron yield to the $2s^2 2p^4(^3P)3s(^2P)$ ionic state at 0° and 54.7°, and derived β values (β is set to -1 and the error bar is not shown when the intensity at 0° was at the noise level).

In order to back up, with explicit theoretical calculations, our assertion that even lower-n resonances can mix significantly with triplet states, we first performed a multiconfiguration Hartree-Fock calculation for the $2p^4(^3P)3p(^2P)5d(^1P_1, ^3P_1, ^3D_1)$ resonances, using Froese Fischer's code [12]. The computed LS-coupled energy values and jj-coupled mixing coefficients c_i in the (predominantly $^1P_1$) eigenvector are given in Table I. Even though the spin-orbit interaction energy $\langle j|H_{\mathrm{SO}}|i\rangle$ is found to be roughly 10–15 meV, the equally small 12 meV energy difference between the $^1P_1$ and $^3D_1$ states causes substantial mixing. Furthermore, large-scale R-matrix calculations, currently in progress, predict a significant cross section at $\theta = 0°$ *only* when mixing with the triplet-state resonances is included [13].

As a final diagnostic, the photoelectron yield along each of the two fine-structure-split vertical lines in Fig. 1(c) is obtained to give partial cross sections to the $3/2$ and $1/2$ levels (see Fig. 3). Now it can be seen more

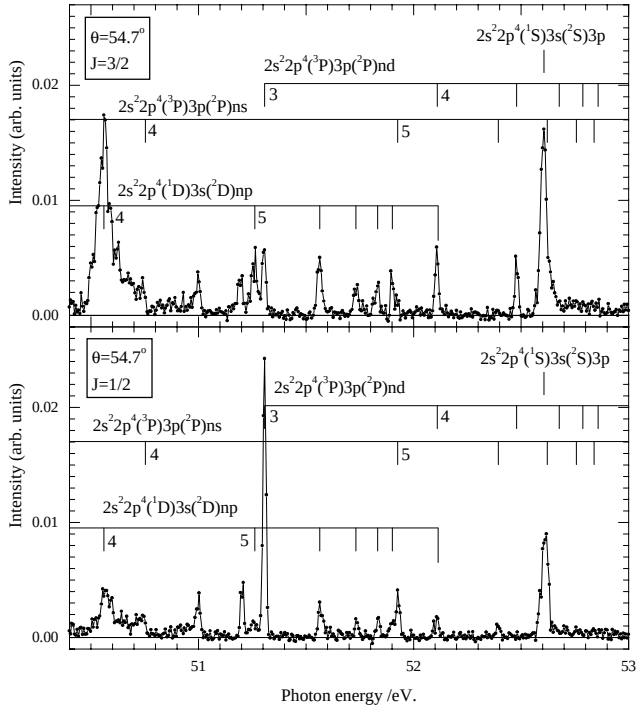

FIG. 3. Photoelectron yield to the $2s^2 2p^4(^3P)3s(^2P_{3/2,1/2})$ fine structure levels at 54.7°.

quantitatively which resonances exhibit LS-forbidden ratios $r \neq 2$. In particular, the $2p^4(^1D)3s(^2D)4p$ and $2p^4(^3P)3p(^2P)3d$ resonances show ratios $r = 4.3$ and $r = 0.2$, respectively. We note that similar ($r \neq 2$) behavior was observed in the ratios of the $np_{3/2}^{-1}$ and $np_{1/2}^{-1}$ fine-structure levels in krypton ($n = 4$) and xenon ($n = 5$) [14], for instance, where spin-orbit effects are expected to be stronger than in the present case. The present high-resolution measurements, on the other hand, allow separation of the $3/2$ and $1/2$ levels in *neon*, where the splitting is too small to have been observed in previous measurements. Another particularly important point is that the resolution of fine-structure levels may prove to be a more universal means of detecting LS-forbidden behavior. This is because for other (e.g., parity favored) transitions, fluctuations in the 0° cross section are not necessarily due to spin-orbit effects.

In conclusion, we have performed highly detailed measurements of two-electron photoionization processes in neon using an angle-resolved 2D photoelectron imaging technique. A cursory study of the 2D images unambiguously indicated that the photoelectron angular distribution and the fine-structure-resolved partial cross sections of a parity-unfavored transition exhibited new LS-forbidden behavior, namely, the emergence of photoelectrons parallel to the photon polarization axis, and the nonconstant ratio of the $^2P_{3/2}$ to $^2P_{1/2}$ cross sections. Important implications of these findings are twofold. First, viewing 2D photoionization images at various angles can permit the easy identification of many unexpected (e.g., LS-forbidden) features that might be overlooked using less-detailed probing techniques. Second, detection of prominent spin-orbit effects means that it is not safe to assume the validity of LS coupling, even for low-lying resonances in a system as light as neon, when performing detailed photoionization studies.

TABLE I. LS-coupled energies (relative to $^1P_1$), and jj-coupled mixing coefficients (including spin-orbit effects) for the (predominantly) $2p^4(^3P)3p(^2P)5d(^1P_1)$ resonance.

LS term	LS energy (eV)	jj Composition
$^3P_1$	−0.010	3%
$^1P_1$	0.000	67%
$^3D_1$	0.012	30%

This work was supported by the U.S. Department of Energy, Office of Basic Energy Science, Division of Chemical Science under Contract No. DE-FG02-95ER14299, and Contract No. DE-FG05-84ER13266 (Z. F.). We thank S. T. Manson and A. F. Starace for several useful discussions.

*Electronic address: Wills@wmich.edu

[1] K. Schulz *et al.*, Phys. Rev. Lett. **77**, 3086 (1996).
[2] K. Codling *et al.*, Phys. Rev. **155**, 26 (1967).
[3] A. A. Wills *et al.*, J. Phys. B **23**, 2013 (1990).
[4] J. A. R. Samson *et al.*, Phys. Rev. A **45**, 259 (1992).
[5] U. Becker *et al.*, Phys. Rev. Lett. **56**, 1120 (1986).
[6] K. Schulz *et al.*, Phys. Rev. A **54**, 3095 (1996).
[7] A. F. Starace, *Theory of Atomic Photoionization, Handbuch der Physik*, edited by W. Mehlhorn (Springer, Berlin, 1982), pp. 1–121.
[8] U. Fano and D. Dill, Phys. Rev. A **6**, 185 (1972).
[9] D. Dill and U. Fano, Phys. Rev. Lett. **29**, 1203 (1972).
[10] N. Berrah *et al.*, J. Phys. B **29**, 5351 (1996); B. Langer *et al.*, in *Proceedings of the Atomic Physics with Hard X-rays from High Brilliance Synchrotron Light Sources Workshop*, ANL/APS/TM-16 (ANL, Argonne, IL, 1996), p. 245.
[11] M. D. Lindsay *et al.*, Phys. Rev. A **45**, 231 (1992).
[12] C. Froese Fischer, Comput. Phys. Commun. **64**, 369 (1991).
[13] T. W. Gorczyca, Z. Felfli, and H. L. Zhou (unpublished).
[14] M. G. Flemming *et al.*, Phys. Rev. A **44**, 1733 (1991).